Wp index: A new substorm index derived from high-resolution geomagnetic field data at low latitude

AUTHOR(S):

Nosé, M.; Iyemori, T.; Wang, L.; Hitchman, A.; Matzka, J.; Feller, M.; Egdorf, S.; ... Curto, J. J.; Segarra, A.; Çelik, C.

CITATION:

Nosé, M. ...[et al]. Wp index: A new substorm index derived from high-resolution geomagnetic field data at low latitude. Space Weather: The International Journal of Research and Applications 2012, 10(8): S08002.

ISSUE DATE:

2012

URL:

http://hdl.handle.net/2433/162016

SPACE WEATHER, VOL. 10, S08002, doi:10.1029/2012SW000785, 2012

Wp index: A new substorm index derived from high-resolution geomagnetic field data at low latitude

M. Nosé,[1] T. Iyemori,[1] L. Wang,[2] A. Hitchman,[2] J. Matzka,[3] M. Feller,[4]
S. Egdorf,[4] S. Gilder,[4] N. Kumasaka,[5] K. Koga,[6] H. Matsumoto,[6] H. Koshiishi,[6]
G. Cifuentes-Nava,[7] J. J. Curto,[8] A. Segarra,[8] and C. Çelik[9]

[1]Data Analysis Center for Geomagnetism and Space Magnetism, Graduate School of Science, Kyoto University, Kyoto, Japan.
[2]Geoscience Australia, Canberra, Australia.
[3]DTU Space, National Space Institute, Technical University of Denmark, Copenhagen, Denmark.
[4]Geophysical Observatory Fürstenfeldbruck, Department of Earth and Environmental Sciences, Ludwig Maximilians Universität, Munich, Germany.
[5]Kakioka Magnetic Observatory, Japan Meteorological Agency, Ibaraki, Japan.
[6]Aerospace Research and Development Directorate, Japan Aerospace Exploration Agency, Ibaraki, Japan.
[7]Instituto de Geofisica Universidad Nacional Autonoma de Mexico, Mexico City, Mexico.
[8]Observatori de l'Ebre (OE), CSIC - Universitat Ramon Llull, Roquetes, Spain.
[9]Kandilli Observatory and Earthquake Research Institute, Boğazici University, Istanbul, Turkey.

Abstract.
Geomagnetic fiel data with high time resolution (typically 1 s) have recently become more commonly acquired by ground stations. Such high time resolution data enable identifying Pi2 pulsations which have periods of 40-150 s and irregular (damped) waveforms. It is well-known that pulsations of this type are clearly observed at mid- and low-latitude ground stations on the nightside at substorm onset. Therefore, with 1-s data from multiple stations distributed in longitude around the Earth's circumference, substorm onset can be regularly monitored. In the present study we propose a new substorm index, the Wp index (Wave and planetary), which reflect Pi2 wave power at low-latitude, using geomagnetic fiel data from 11 ground stations. We compare the Wp index with the AE and ASY indices as well as the electron flu and magnetic fiel data at geosynchronous altitudes for 11 March 2010. We fin that significan enhancements of the Wp index mostly coincide with those of the other data. Thus the Wp index can be considered a good indicator of substorm onset. The Wp index, other geomagnetic indices, and geosynchronous satellite data are plotted in a stack for quick and easy search of substorm onset. The stack plots and digital data of the Wp index are available at the web site (http://s-cubed.info) for public use. These products would be useful to investigate and understand space weather events, because substorms cause injection of intense flu es of energetic electrons into the inner magnetosphere and potentially have deleterious impacts on satellites by inducing surface charging.

1. Introduction

Substorms are one of the most conspicuous phenomena in space physics. A substorm releases a large amount of electromagnetic energy stored in the magnetotail into the ionosphere and the inner magnetosphere in a short time scale of minutes. Their occurrence gives rise to a number of different events, including auroral breakup, energetic particle injection in the inner magnetosphere, magnetic fiel dipolarization, bursty bulk plasma fl w in the plasma sheet, magnetic reconnection in the magnetotail, and plasmoid development in the distant tail. Substorms also cause disturbances in the ground-based geomagnetic field that is, high-latitude negative bays and mid-latitude positive bays. In order to measure substorm activities, geomagnetic indices that reflec the occurrence of high-latitude negative bays and mid-latitude positive bays have been invented: the AE (Auroral Electrojet) index for the former [*Davis and Sugiura*, 1966] and the ASY (ASYmmetric disturbance) index for the latter [*Iyemori and Rao*, 1996]. These indices are derived from data collected by multiple stations distributed around the globe at different longitudes. Data from 12 stations and 6 stations contribute to the AE index and the ASY index, respectively. Thus these indices are considered sensitive to high-latitude negative bays or mid-latitude positive bays at any given UT time, although magnetic bays are local phenomena that appear predominantly on the nightside. Hence, the AE and ASY indices are widely used to identify the occurrence of substorms.

"Pi2 pulsations" designate a type of geomagnetic fiel oscillations that have an irregular (damped) waveform and a period in the range of 40-150 s [*Jacobs et al.*, 1964]. Early studies reported that Pi2 pulsations can be clearly observed at low- and mid-latitude ground stations on the nightside, when high-latitude negative bays or mid-latitude positive bays are initiated [*Saito et al.*, 1976a, b; *Sakurai and Saito*, 1976a]. They also appear almost simultaneously with auroral breakups [e.g., *Sakurai and Saito*, 1976a; *Gelpi et al.*, 1987], energetic particle injection in the inner magnetosphere [e.g., *Yeoman et al.*, 1994; *Saka et al.*, 1996], and magnetic fiel dipolarization [e.g., *Sakurai and McPherron*, 1983; *Yumoto et al.*, 1989].

Since low-latitude Pi2 pulsations exhibit greatest power near midnight, multiple ground stations distributed longitudinally around the globe are needed for their detection at any given UT time.

Recent advancements in computers and instrumentation for geomagnetic field measurements enable a large number of geomagnetic stations to record geomagnetic field variations with a time resolution of 1 s. These developments facilitate the derivation of a new index measuring Pi2 power. Such an index would be useful and convenient to identify the occurrence of substorms similar to the AE and ASY indices. In this study, using data from a longitudinal network of 11 ground stations, we propose a new substorm index, the "Wp index" (Wave and planetary). This is an extension of the work of *Nosé et al.* [2009], in which only data from five ground stations were used and preliminary results were presented. We improve the derivation procedure of the Wp index introduced by *Nosé et al.* [2009]. To extend the evaluation of this new substorm index beyond our previous study, we also compare the Wp index with particle and magnetic field data from geosynchronous satellites. Thus, the present study supersedes their work.

From the viewpoint of space weather, substorms are important research topics because they can cause satellite anomalies. Substorms produce energetic electrons with energies in the range of several to several hundreds of keV that are often responsible for surface charging of satellites, leading to electrostatic discharge and possible damage to satellite electronics [e.g., *Fennell et al.*, 2001]. Surface charging is reported to occur mostly in the 2300 to 0600 LT region at geosynchronous altitude [*McPherson et al.*, 1975; *Koons and Gorney*, 1992], which is consistent with the path of substorm-injected energetic electrons drifting eastward from the near-Earth magnetotail. A recent well-known satellite anomaly is the Galaxy 15 geosynchronous telecommunication satellite which stopped responding to commands from the ground controller at 0948 UT on 5 April 2010. Galaxy 15 began to wander away from its orbital position causing a risk of collision with other geosynchronous satellites. This satellite anomaly was attributed to significant electron injection associated with large substorms and the unfortunate positioning of Galaxy 15 around the hazardous midnight-to-dawn sector at the time of the substorms [*Allen*, 2010; *Connors et al.*, 2011]. More examples of satellite anomalies due to substorm-associated electron injection are compiled by *Bedingfield et al.* [1996]. The substorm indices including AE, ASY, and Wp would help better characterize space weather events and aid in the mitigation of harmful impacts on satellites.

This paper is organized as follows. In section 2, we describe the longitudinal network of ground stations used to derive the Wp index. Section 3 elucidates the method for calculating the Wp index by employing wavelet analysis. Section 4 presents an example of Wp calculation for 11 March 2010. In section 5, the Wp index is compared with the AE and ASY indices and geosynchronous satellite data to verify whether it is a good indicator of substorm activity. Section 6 introduces a web-based product for quick and easy search of substorm onset based on the database of the Wp index and other substorm indicators. Finally, section 7 gives a summary of this paper.

2. Longitudinal Network of Ground Stations for Wp Index

Figure 1 shows the locations of 11 ground stations in geomagnetic coordinates that were used to derive the Wp index. Dotted blue circles indicate geomagnetic latitudes (GMLAT) of 20° and 50°. The coordinates of the stations are listed in Table 1. The 11th Generation IGRF is used to calculate geomagnetic coordinates. The station names (3-letter abbreviation code, sponsoring country) are Tuscon (TUC, United States), Honolulu (HON, United States), Canberra (CNB, Australia), Kakioka (KAK, Japan), Learmonth (LRM, Australia), Urumqi (WMQ, China), Iznik (IZN, Turkey), Fürstenfeldbruck (FUR, Germany), Ebro (EBR, Spain), Tristan da Cunha (TDC, Denmark), and San Juan (SJG, United States). Since CNB, LRM, and TDC are located in the southern hemisphere, their locations are plotted as geomagnetically conjugate points in Figure 1. The absolute values of the geomagnetic latitude of these 11 stations range between 21° and 49°. The largest longitudinal separation between the stations is about 52° (between WMQ and IZN). Therefore, the longitudinal network of these stations is sufficiently dense such that at least one station is always positioned on the nightside where low-latitude Pi2 pulsations can be clearly observed.

3. Method of Derivation of Wp Index

3.1. Wavelet Analysis

In deriving the Wp index we use wavelet analysis, in which a time series is decomposed into orthonormal basis functions that are localized in time and limited to a specific frequency range (wavelets). Thus, wavelet analysis is suitable for investigating the wave power of phenomena that are limited in both time and frequency, such as Pi2 pulsations. The time series is mapped to the time-frequency domain; therefore, the wavelet transform has two parameters that correspond to time and frequency. For a time series $x(t)$, the wavelet transform is expressed as

$$x(t) = \sum_j \sum_k \alpha_{j,k} \cdot \psi_{j,k}(t), \tag{1}$$

$$\alpha_{j,k} = \int_{-\infty}^{\infty} x(t) \cdot \psi^*_{j,k}(t) dt, \tag{2}$$

where $\alpha_{j,k}$ is the wavelet coefficient, $\psi_{j,k}(t)$ is the discrete wavelet set, and the asterisk denotes the complex conjugate. $\psi_{j,k}(t)$ is constructed from an analyzing wavelet $\phi(t)$, which generates the orthonormal wavelet set, by

$$\psi_{j,k}(t) = \phi(2^j t - k), \tag{3}$$

where j and k are integers. This equation indicates that j is related to the dilation or contraction of $\psi(t)$ and k is related to the shift of $\psi(t)$ in the time domain. Thus, j and k can be considered parameters of frequency (dilation) and time (translation), respectively. In this study we use the Meyer wavelet [*Meyer*, 1989] as an analyzing wavelet, because the Meyer wavelet is band-limited in frequency [e.g., *Sasaki et al.*, 1992; *Sato and Yamada*, 1994; *Yamada and Ohkitani*, 1991; *Yamanaka et al.*, 1994; *Yomogida*, 1994] as are Pi2 pulsations (i.e., 6.67-25.0 mHz).

For actual analysis, we use a discrete time series and take a finite data segment. Assuming a time series that has a sampling rate dt and number of data points N ($N = 2^n$, n is an integer), we will obtain wavelet coefficients $\alpha_{j,k}$ confined to $0 \le j \le n-1$ and $0 \le k \le 2^j - 1$. The frequency band for each j is $2^j/3T \le f \le 2^{j+2}/3T$, where T is the data length $T = Ndt$. A more detailed description of wavelet analysis can be found in *Nosé et al.* [1998].

3.2. Derivation Procedure

Using the 1-s geomagnetic field data from the 11 stations, we calculate the Wp index as follows. A schematic figure of the derivation procedure is shown in Figure 2.

1. The magnetic field in the horizontal plane is converted into H_N-H_E coordinates, where the H_N and H_E components are parallel and perpendicular to the local magnetic field, respectively. The H_E component is positive eastward. The orientation of the local magnetic field (i.e., declination) at each station is calculated by using the 11th Generation IGRF. Table 1 lists the declination on 1 January 2005, which is applied to the subsequent periods. In the derivation of the Wp index, only the H_N component is used (Figure 2a), because the low-latitude Pi2 amplitude in the H_N component is much less dependent on GMLAT than that in the H_E component [*Yumoto et al.*, 1994; *Allan et al.*, 1996].

2. Wavelet analysis is applied to geomagnetic field data for a segment of 512-s length. The data segment is then shifted forward by 60 s and wavelet analysis is repeated (Figure 2b). The frequency

bands of the wavelet functions with j=4 and 5 are 5.2-20.8 mHz and 10.4-41.7 mHz, respectively, which cover the frequency range of Pi2 pulsations (6.67-25.0 mHz). The wavelet coefficients of j=4 and 5 ($\alpha_{4,k}$ and $\alpha_{5,k}$) are computed so that their magnitudes represent the maximum amplitude of the corresponding wavelet functions in nT. (Careful readers may notice that the frequency bands of the wavelet function are derived for the case of N=1024. This is because 256 artificial data points are added at both ends of the 512-s data segment before wavelet analysis. The artificial points added to the beginning of the data segment have the same value as the first data point and those added to the end of the data segment have the same value as the last data point.)

3. Using the obtained wavelet coefficients, we calculate wavelet power with a time resolution of 1 min (Figure 2c). Wavelet power is defined as an average of the wavelet coefficients of j=4 and 5 ($\alpha_{4,k}$ and $\alpha_{5,k}$) in a given 1-min bin. This process results in a time series of 1-min wavelet power (i.e., 1440 data points/day) for each station, which is named the W_{ABB} index, where "W" stands for "Wave" and "ABB" is the 3-letter abbreviation code of the station.

4. The Wp index is derived from the W_{ABB} indices at 11 stations. Since Pi2 pulsations have dominant power on the nightside, we use only the W_{ABB} indices from the stations located at 1800-0400 MLT. The Wp index is simply defined as an average of the W_{ABB} indices of the stations in this MLT range (Figure 2d).

4. Example of Calculation of Wp Index for 11 March 2010

4.1. One-second Geomagnetic Field Data

Following the procedure described in the previous section, we calculate the Wp index for 11 March 2010, using data from the 11 ground stations. Figure 3 displays the 1-s geomagnetic field data in the H_N component from the 11 stations for time intervals of 0500-0600 UT, 0820-0920 UT, 1110-1210 UT, and 1740-1840 UT on 11 March 2010. MLT of each station at the beginning of the time interval is indicated at the bottom-left corner of each panel. In Figure 3a, Pi2 pulsations accompanied by positive bays are identified at TUC and SJG around 0535 UT, when both stations are located close to midnight (MLT∼21-01 hr). Simultaneously, there are also Pi2 pulsations at other stations, although their amplitudes are generally smaller and they are accompanied by no clear positive bays. Note that the Pi2 pulsations are preceded by another Pi2 activity at SJG and TUC around 0525 UT, although it has a smaller amplitude and no positive bay. Such an intermittent appearance of Pi2 pulsations is a typical feature known as "a pulsation train (Pt)" or "a Pi2 train" [e.g., *Saito et al.*, 1976b; *Sakurai and Saito*, 1976b; *Sergeev et al.*, 1986; *Sutcliffe and Lyons*, 2002]. In Figure 3b, CNB, HON, and TUC observed Pi2 pulsations at 0852-0900 UT. These three stations are located near midnight (MLT∼19 hr, ∼22 hr, and ∼01 hr). Other stations located on the dayside or in the early morning sector observed no clear appearance of Pi2 pulsations. In Figure 3c, LRM, KAK, CNB, and HON observed Pi2 pulsations at 1138 UT and 1144 UT near midnight (MLT∼19-01 hr). The latter pulsations are accompanied by clear positive bays. Therefore this event is considered a Pi2 train. On the dayside, magnetic field fluctuations with larger amplitude appear at FUR and EBR around 1140 UT. However, their waveforms seem to be different from those of the nightside Pi2 pulsations. Moreover, they started from 1141 UT, which does not coincide with the onset time of the nightside Pi2 pulsations. The results indicate no direct connection between the dayside magnetic field fluctuations and Pi2 pulsations. In Figure 3d, Pi2 pulsations (or a Pi2 train) can be found at almost all 11 stations at 1805-1810 UT and 1814-1820 UT. The amplitude of these pulsations is the largest at stations near local midnight, that is, FUR (MLT∼19.5 hr), IZN (MLT∼20.5 hr), WMQ (MLT∼0.0 hr), and LRM (MLT∼1.5 hr). Positive bays are clearly evident at WMQ and LRM for the second Pi2 pulsation.

The above results regarding the MLT dependence of Pi2 occurrence are consistent with previous results; that is, Pi2 pulsations are frequently observed near midnight (2100-0100 MLT) [e.g., *Saito and Matsushita*, 1968; *Smith*, 1973; *Sakurai and McPherron*, 1983; *Singer et al.*, 1983].

4.2. W_{ABB} Index

Following procedures 2 and 3 described in section 3.2, we apply wavelet analysis to the geomagnetic field data for 11 March 2010 and compute the W_{ABB} indices. Results are displayed with red lines in the top 11 panels of Figure 4. A horizontal black bar in each panel indicates local nighttime (1800-0400 MLT) at the station. The four time intervals of Figure 3 are shown with horizontal light-blue bars. It is worth mentioning briefly here the W_{ABB} indices during local daytime. Base values of the W_{ABB} indices at daytime (i.e., the periods without horizontal black bars) are generally larger than those at local nighttime, in particular, at higher latitude stations (CNB, FUR, and EBR). This is probably because the daytime is rich in activities of geomagnetic Pc3-4 pulsations, which have wave periods similar to Pi2 but are caused by upstream waves in the solar wind [*Yumoto*, 1986; *Odera*, 1986; *Verö*, 1986]. Thus, the W_{ABB} indices at daytime have contributions from Pc3-4 pulsations to some extent. The amplitudes of Pc 3-4 pulsations become larger at higher latitudes [e.g., *Matsuoka et al.*, 1997], resulting in the larger base values at CNB, FUR, and EBR.

In the first time interval of 0500-0600 UT, clear enhancements of W_{TUC} and W_{SJG} can be seen; this is consistent with Figure 3a. Other stations also show increases of the W_{ABB} indices, although they are smaller than those of W_{TUC} and W_{SJG}, except for CNB. (It seems that CNB, located at higher latitude, observed Pc-type pulsations before 0530UT and this Pc-type wave activity may be further stimulated by the substorm onset at 0535 UT.) In the second time interval of 0820-0920 UT, there are sudden increases in W_{CNB}, W_{HON}, and W_{TUC}, which reflect the appearance of Pi2 pulsations as seen in Figure 3b. We can even observe enhancements of the W_{ABB} indices in the afternoon sector (KAK, LRM, WMQ, IZN, and FUR), but they are less significant than the nighttime enhancements. In the third time interval of 1110-1210 UT, we notice clear enhancements of W_{LRM}, W_{KAK}, W_{CNB}, and W_{HON}, which are consistent with our findings in Figure 3c. There are sharp increases in W_{FUR} and W_{EBR} in the local daytime; but, as we discussed in section 4.1, they are not related to Pi2 activities. In the fourth time interval of 1740-1840 UT, we find enhancements of the W_{ABB} indices at all stations, although larger enhancements are found on the nightside (FUR, IZN, WMQ, and LRM), being consistent with the visual inspection of the geomagnetic field data shown in Figure 3d.

4.3. Wp Index

From the W_{ABB} indices, we calculate the Wp index by procedure 4. The result of the calculation is shown with the blue lines in the bottom panel of Figure 4. We can see significant increases of the Wp index around 0535 UT, 0850 UT, 1140 UT, and 1805 UT during the four time intervals designated by the horizontal light-blue bars. Close inspection reveals that the increases of the Wp index around 0535 UT, 1140 UT, and 1805 UT are composed of two peaks corresponding to the Pi2 trains identified in Figures 3a, 3c, and 3d. The Wp index, therefore, can be thought as "a global index" that reflects the nighttime low-latitude wave power in the Pi2 frequency range at any given UT time.

5. Wp Index as a Good Indicator of Substorm Activity

5.1. Comparison with Other Substorm Signatures: Case Study for 11 March 2010

Now we compare substorm signatures found in the Wp index and those found in the AE index, the ASY index, and geosynchronous satellite data. First, we examine whether the AE and ASY indices showed substorm signatures in the aforementioned four time intervals. For comparison among geomagnetic indices,

we display plots of the AE, -AL, ASY-H, ASY-D, and Wp indices for 11 March 2010 in the top five panels of Figure 5. The Wp index in the fifth panel is identical to that in the bottom panel of Figure 4. Enhancement of the Wp index is considered as being due to the occurrence of a Pi2 pulsation at low-latitude, while increases of the AE, -AL, ASY-H, and ASY-D indices are interpreted as the occurrence of high-latitude negative bays and mid-latitude positive bays. For the Wp increase at 0535 UT, all other indices (AE, -AL, ASY-H, and ASY-D) also increase. Around 0850 UT, the AE and -AL indices are clearly enhanced. Around 1140 UT when the Wp index shows an enhancement, the AE and -AL indices show minor increases. The Wp enhancement around 1805 UT is accompanied by enhancements of the AE, -AL, and ASY-H indices. The comparison reveals good correspondence between the Wp index and other geomagnetic indices in terms of the detection of substorm occurrence.

Second, in order to further confirm the value of the Wp index as a substorm index, we examine the high-energy (590-1180 keV) electron flux measured by the standard dose monitor (SDOM) onboard the Data Relay Test Satellite (DRTS) [*Matsumoto et al.*, 2001] and the magnetic field measured by the magnetometer (MAM) onboard the Engineering Test Satellite (ETS)-VIII [*Koga and Obara*, 2008], both of which are geosynchronous satellites launched by Japan Aerospace Exploration Agency (JAXA). The DRTS electron flux data are shown in the sixth panel of Figure 5. In the bottom three panels of Figure 5, the ETS-VIII magnetic field data are shown in *PEN* coordinates, where H_p is perpendicular to the satellite orbital plane and directed northward, H_e is parallel to the satellite-Earth line and points earthward, and H_n is perpendicular to both H_p and H_e and points eastward. Open and closed circles in these panels indicate local noon and local midnight at the satellite longitude. The DRTS data show that electron flux enhancements (i.e., particle injection in the magnetosphere) occur around the time of the four Wp index enhancements ($\sim$0530 UT, $\sim$0900 UT, $\sim$1200 UT, and $\sim$1815 UT). The ETS-VIII satellite observes temporary drops in H_p and H_e followed by increases around the same time. (Variations around 1800 UT are not clear, because the satellite moves to the early morning sector where it is probably far from the substorm onset meridian.) Since the ETS-VIII satellite is located below the geomagnetic equator at -7.8° GMLAT, the observed H_p and H_e variations are interpreted to be magnetic field stretching followed by magnetic field dipolarization. Therefore, the Wp enhancements in the four time intervals also correspond to the substorm signatures in the magnetosphere.

Enhanced activities of the Wp index can also be seen in other time intervals. At 0000-0100 UT, there are three intermittent increases of the Wp index, which can be considered a Pi2 train. It seems that one of the three Wp increases (possibly the second increase around 0020 UT) is accompanied by clear enhancements of the AE, -AL, ASY-H, and ASY-D indices, being similar to the Pi2 trains around 0535 UT, 1140 UT, and 1805 UT. We can see minor enhancements of the Wp index at 1450 UT, 1600 UT, 1700 UT, 1720 UT, and 1950 UT, none of which are associated with enhancements of the AE and ASY indices, energetic electron injection, or magnetic field dipolarization. This may be caused by insensitivity of the AE and ASY indices and geosynchronous satellite data to small substorm onsets or pseudo-substorm onsets, which are followed by no global development of activities [e.g., *Akasofu*, 1964; *Ohtani et al.*, 1993]. On the other hand, the Wp index, which reflects low-latitude Pi2 pulsations, is sensitive to such substorm onsets [e.g., *Sakurai and Saito*, 1976a].

The above arguments confirm that the significant enhancements of the Wp index are usually accompanied by other substorm signatures. It seems that the subsidiary enhancements of the Wp index indicate small substorm or pseudo-substorm onsets. Therefore, we conclude that the Wp index is a useful index to detect substorm onset.

5.2. Comparison with Other Substorm Signatures: Statistical Study

We statistically compare substorm signatures between the Wp index and other substorm indices/geosynchronous satellite data for a 1 month interval of March 2010. The comparison is made in two different ways. In the first way, we make an event list of Wp enhancement, and then check whether the listed Wp enhancement is accompanied by other substorm signatures. The second way uses the AE index to identify substorm onset. Then we examine whether the substorm onset selected by the AE index is associated with Wp enhancement.

5.2.1. Events Selected by Wp Index

Onset time of enhancement in the Wp index (t_0) is selected by using the following criteria: (1) the standard deviation of the Wp index in a 30-min interval before t_0 is $\leq$0.05 nT; and (2) the Wp index is enhanced to $\geq$0.4 nT within 10 min after t_0. Criterion 1 is applied to require quiescence of geomagnetic activity before the onset. These criteria sometimes yield a consecutive series of onset times, like t_0=T, T+1 min, $\cdots$, T+k min. In this case, we take the last onset time, that is, t_0=T+k min, and discard the others. The above selection procedure identifies 64 events of Wp enhancement in March 2010, which are listed in Table 2. Note that all 4 distinct events of 11 March 2010 discussed in section 5.1 are successfully selected as t_0=0527 UT, 0853 UT, 1137 UT, and 1804 UT.

Then we examine whether other substorm indices/geosynchronous satellite data show substorm signatures after t_0. Regarding other substorm indices, we calculate relative variations after t_0 by $\Delta S(t)$=$S(t) - \frac{1}{5}\sum_{i=1}^{5} S(t_0 - i \text{ min})$, where S is AE, -AL, ASY-H, or ASY-D, and $t \geq t_0$. If the maximum value of ΔAE(t) or -ΔAL(t) within a period of t=$t_0 \sim t_0 + 60$ min is larger than 75 nT, we consider that a substorm signature (i.e., a high-latitude negative bay) is evident. For ΔASY-H(t) or ΔASY-D(t), we identify a substorm signature (i.e., a mid-latitude positive bay) if the maximum value is larger than 10 nT. These thresholds are chosen as the judgement based on them is consistent with the visual inspection for the 4 events of 11 March 2010 done in section 5.1. For the geosynchronous satellite data, it is found difficult to determine a fixed threshold to identify substorm signatures, because increases of the energetic electron flux and the magnetic field depend on local time of satellites, as can be seen in Figure 5. Therefore we visually examine the DRTS and ETS-VIII data to identify substorm signatures (i.e., particle injection and magnetic field dipolarization in the magnetosphere). Results of the examination are compiled in Table 2. "Y" and "N" denote the presence and absence of substorm signatures after t_0, respectively. An asterisk (*) indicates that the geosynchronous satellite is located on the dayside, where it is inappropriate to observe substorm signatures (i.e., 0000-1200 UT for DRTS and 2000-0800 UT for ETS-VIII).

In Table 2, we count the number of events including at least one Y or Y*, and find 50 such events (checkmarks in the 2nd right column in Table 2). That is, 78% (=50/64) of the Wp enhancements are followed by a substorm signature. If we take N* events into consideration; that is, if we consider the possibility of missing substorm signatures because of unsuitable location of satellites to detect them, we find 59 events including Y or Y* or N* (checkmarks in the rightmost column in Table 2). Then the percentage possibly becomes higher up to 92% (=59/64). This statistical result also confirms that the enhancements of the Wp index are usually (78-92%) accompanied by other substorm signatures.

There are 14 events where the Wp index is enhanced while no other substorm signatures are identified (no checkmarks in the 2nd right column in Table 2). We visually inspect the 1-s geomagnetic field data from the 11 stations for the 14 events, and confirm that Pi2 pulsations obviously appear on the nightside for all of the events. (Plots are available as an online supplemental figure.) The 14 events are probably small substorm onsets or pseudo-substorm onsets, and we believe that the arguments in section 5.1 are supported by the statistical study.

Table 3 summarizes the number of events in classification categories of Y/Y*/N/N*. We find that the Wp enhancement is associated with enhancements of the AE or -AL index $\sim$70% (=45/64 or 44/64) of the events, and with enhancements of the ASY-H

or ASY-D index ∼30% (=22/64 or 16/64) of the events. Comparison with geosynchronous satellite data reveals that Wp enhancement is accompanied by electron flux enhancements on 27% (=(12+5)/64) of occasions and by magnetic field dipolarization on 30% (=(17+2)/64) of occasions. If we include N* events in the satellite statistics, the percentages possibly increase up to 50-64% (=(12+5+15)/64 or (17+2+22)/64). The differences in the percentages among the AE and ASY indices and geosynchronous satellite data may be due to their different sensibility to substorms.

5.2.2. Events Selected by AE Index

Using the AE index, we select substorm onset that satisfies the following criteria: (1) the standard deviation of the AE index in a 30-min interval before onset time (t_0') is $\leq$ 10 nT; and (2) within 20 min after t_0', the AE index is increased by $\geq$150 nT from quiet value, which is the mean of the AE index during 30 min before t_0'. When the above criteria find a consecutive series of onset times, we take only the last one and ignore the others in the similar way as section 5.2.1. From this selection procedure we identify 24 substorm events in March 2010, which are listed in Table 4.

For the 24 events, we examine whether the Wp index is enhanced in a time interval between $t_0'-10$ min and $t_0'+20$ min. Start of the time interval (i.e., $t_0'-10$ min) is decided so, because the onset time of AE increase is likely to be delayed against actual substorm onset time when substorm initiates in the longitudinal sector between AE stations. It is found that 15 events of AE increase are accompanied by sudden enhancements of the Wp index with peak values of $\geq$0.4 nT, which are labeled A in Table 4. There are 8 events of AE increase that are associated with sudden Wp enhancements with peak values of 0.2-0.4 nT (label B in Table 4). The rest of them, that is, an event of t_0'=1437 UT on 8 March 2010 labeled C in Table 4, also coincides with an abrupt Wp enhancement, though its peak value is ∼0.13 nT. Therefore we conclude that the substorm events identified by the AE index are almost completely associated with the Wp enhancements.

5.3. Different Behavior of Geomagnetic Indices at Substorm Onset

Since the Wp/AE/ASY indices reflect different substorm signatures, it is natural that their behaviors or time scales of variations at substorm onset are different from each others. For instance, the Wp index increases in a short time (∼10 min) at substorm onset and returns to its initial values within a few tens of minutes, whereas the AE and ASY indices continue to increase for a few tens of minutes to an hour after substorm onset and decay in the order of 1 hour. These different behaviors can be clearly seen in the 0535 UT and 1805 UT substorm events in Figure 5. As discussed in section 5.1 and 5.2, there is also the difference in sensitivity to substorm onset among these indices.

5.4. Magnitude of Wp Index

According to the derivation procedure of the Wp index, its magnitude can be regarded as the average amplitude of low-latitude Pi2 pulsations on the nightside. Recent studies by *Takahashi et al.* [2002] and *Takahashi and Liou* [2004] reported a generally positive correlation between the auroral power and low-latitude Pi2 amplitude at Kakioka. The Pi2 amplitude is typically 0.05 nT for an auroral power of 1 GW and 0.5 nT for an auroral power of 50 GW, when both Pi2 and peak auroral power occur in the 22-01 MLT sector. *Rae et al.* [2011] reported that the magnetic field fluctuations in the Pi2 period band have more pronounced power for substorms than for pseudo-substorms. (They however used ground station data not from low-latitude but from auroral latitude.) Thus it may be possible that the magnitude of the Wp index is related to the substorm size; future studies will include investigation of their relation.

6. "Substorm Swift Search" Web Site: Daily Stack Plots and Digital Data of Wp

We create daily stack plots displaying the AE, ASY, and Wp indices as well as the high-energy electron flux measured by DRTS/SDOM and the magnetic field measured by ETS-VIII/MAM (similar to Figure 5). Such daily stack plots are useful for users to search for substorm onsets swiftly from five different viewpoints, that is, high-latitude negative bay, mid-latitude positive bay, low-latitude Pi2 pulsation, energetic electron injection, and magnetic field dipolarization. The stack plots are available at a web site called "Substorm Swift Search (S^3, S-cubed)" (http://s-cubed.info). Digital data of the Wp index and the W_{ABB} indices can also be downloaded from the web site for public use.

7. Summary

We propose a new substorm index, the Wp index (Wave and planetary), using geomagnetic field data with a time resolution of 1 s from 11 low-latitude stations (i.e., Tucson, Honolulu, Canberra, Kakioka, Learmonth, Urumqi, Iznik, Fürstenfeldbruck, Ebro, Tristan da Cunha, and San Juan). The Wp index is related to the wave power of low-latitude Pi2 pulsations. In deriving the Wp index, we employ wavelet analysis which is suitable for investigating the power of short-lived waves, such as Pi2 pulsations. The above 11 stations are distributed around the globe at different longitudes with the maximum separation between two neighboring stations of about 52° (between Urumqi and Iznik). Thus, at least one station is always located on the nightside where Pi2 pulsations have dominant power. Since we use only geomagnetic stations on the nightside (1800-0400 MLT) for calculating the Wp index, this index can be considered "a global index" reflecting Pi2 wave power during local nighttime at any given UT time.

We compare substorm occurrence estimated from the Wp index and those from the AE and ASY indices as well as geosynchronous satellite data for 11 March 2010. Significant enhancements of the Wp index (low-latitude Pi2 pulsations) mostly coincide with increases of the AE and -AL indices (high-latitude negative bays), increases of the ASY-H and ASY-D indices (mid-latitude positive bays), electron flux enhancements at the DRTS satellite (particle injection in the magnetosphere), and magnetic field increases in the northward and earthward components at the ETS-VIII satellite (magnetic field dipolarization in the magnetosphere). This is also confirmed by a statistical study for a 1 month interval of March 2010. We demonstrate that the Wp index is a good indicator of substorm onset.

The Wp index is made available at a web page (http://s-cubed.info) in the form of both plots and digital data. The plots are provided in a stack along with the AE and ASY indices as well as the high-energy electron flux and magnetic field data acquired by geosynchronous satellites. These stack plots make it easier for users to quickly identify substorm occurrence.

In terms of space weather, energetic electrons generated at substorm onset can charge the surfaces of satellites in the magnetosphere. It occasionally happens that surface charging results in electrostatic discharge that couples into satellite electronics and causes satellite operational anomalies. The stack plots including the Wp index, therefore, would also be useful to investigate and understand the satellite anomalies associated with substorms.

Acknowledgments

We are thankful to K. Takahashi and T. Sakanoi for their helpful comments. Thanks are also due to J. J. Love, J. E. Caldwell, and other staff of the USGS Geomagnetism Program for their assistance in processing geomagnetic field data from USGS. This work was supported by the Ministry of Education, Science, Sports, and Culture, Grant-in-Aid for Young Scientists (B) (grant 19740303 and 22740322) and Grant-in-Aid for Scientific Research (B) (grant 22340146). Part of this work was conducted while Masahito Nosé was a visiting scientist at the Johns Hopkins University Applied Physics Laboratory under the support of NSF grant ATM-0646055.

References

Akasofu, S.-I. (1964), The development of the auroral substorm, *Planet. Space Sci.*, *12*, 273–282, doi:10.1016/0032-0633(64)90151-5.

Allan, W., F. W. Menk, B. J. Fraser, Y. Li, and S. P. White (1996), Are low-latitude Pi2 pulsations cavity/waveguide modes?, *Geophys. Res. Lett.*, *23*, 765–768, doi:10.1029/96GL00661.

Allen, J. (2010), The Galaxy 15 anomaly: Another satellite in the wrong place at a critical time, *Space Weather*, *8*, S06008, doi:10.1029/2010SW000588.

Bedingfield, K. L., R. D. Leach, and M. B. Alexander (1996), Spacecraft system failures and anomalies attributed to the natural space environment, *NASA Reference Publication 1390*, NASA Marshall Space Flight Center, Huntsville, AL.

Connors, M., C. T. Russell, and V. Angelopoulos (2011), Magnetic flux transfer in the 5 April 2010 Galaxy 15 substorm: an unprecedented observation, *Ann. Geophys.*, *29*, 619–622, doi:10.5194/angeo-29-619-2011.

Davis, T. N., and M. Sugiura (1966), Auroral electrojet activity index AE and its universal time variations, *J. Geophys. Res.*, *71*, 785–801.

Fennell, J. F., H. C. Koons, J. L. Roeder, and J. B. Blake (2001), Spacecraft charging: Observations and relationship to satellite anomalies, *Aerospace Rep. TR-2001(8570)-5*, Aerospace Corp., El Segundo, CA.

Gelpi, C., W. J. Hughes, and H. J. Singer (1987), A comparison of magnetic signatures and DMSP auroral images at substorm onset - Three case studies, *J. Geophys. Res.*, *92*, 2447–2460, doi:10.1029/JA092iA03p02447.

Iyemori, T., and D. R. K. Rao (1996), Decay of the Dst field of geomagnetic disturbance after substorm onset and its implication to storm-substorm relation, *Ann. Geophys.*, *14*, 608–618, doi:10.1007/s005850050325.

Jacobs, J. A., Y. Kato, S. Matsushita, and V. A. Troitskaya (1964), Classification of geomagnetic micropulsations, *J. Geophys. Res.*, *69*, 180–181, doi:10.1029/JZ069i001p00180.

Koga, K., and T. Obara (2008), Development and measurement result of technical data acquisition equipment (TEDA) onboard ETS-VIII, *IEICE Tech. Rep.*, *108*(100), 23–25, (in Japanese).

Koons, H. C., and D. J. Gorney (1992), The relationship between electrostatic discharges on spacecraft p78-2 and the electron environment, *Aerospace Rep. TR-0091(6940-06)-2*, Aerospace Corp., El Segundo, CA.

Matsumoto, H., et al. (2001), Compact, lightweight spectrometer for energetic particles, *IEEE Trans. Nucl. Sci.*, *48*, 2043–2049, doi:10.1109/23.983170.

Matsuoka, H., K. Takahashi, S. Kokubun, K. Yumoto, T. Yamamoto, S. I. Solovyev, and E. F. Vershinin (1997), Phase and amplitude structure of Pc 3 magnetic pulsations as determined from multipoint observations, *J. Geophys. Res.*, *102*, 2391–2404, doi:10.1029/96JA02918.

McPherson, D. A., D. P. Cauffman, and W. R. Schober (1975), Spacecraft charging at high altitudes: SCATHA satellite program, *J. Spacecraft Rockets*, *12*, 621–626, doi:10.2514/3.57027.

Meyer, Y. (1989), Orthonormal wavelets, in *Wavelets*, edited by J. M. Combes, A. Grossmann, and Ph. Tchamitchian, pp. 21–37, Springer-Verlag, Berlin.

Nosé, M., T. Iyemori, M. Takeda, T. Kamei, D. K. Milling, D. Orr, H. J. Singer, E. W. Worthington, and N. Sumitomo (1998), Automated detection of Pi2 pulsations using wavelet analysis: 1. Method and an application for substorm monitoring, *Earth Planets and Space*, *50*, 773–783.

Nosé, M., et al. (2009), New substorm index derived from high-resolution geomagnetic field data at low latitude and its comparison with AE and ASY indices, in *Proceedings of XIIIth IAGA Workshop on Geomagnetic Observatory Instruments, Data Acquisition, and Processing*, U.S. Geological Survey Open-File Report 2009-1226, edited by J. J. Love, pp. 202–207.

Odera, T. J. (1986), Solar wind controlled pulsations: A review, *Rev. Geophys.*, *24*, 55–74, doi:10.1029/RG024i001p00055.

Ohtani, S., et al. (1993), A multisatellite study of a pseudo-substorm onset in the near-Earth magnetotail, *J. Geophys. Res.*, *98*, 19,355–19,367, doi:10.1029/93JA01421.

Rae, I. J., K. R. Murphy, C. E. J. Watt, and I. R. Mann (2011), On the nature of ULF wave power during nightside auroral activations and substorms: 2. Temporal evolution, *J. Geophys. Res.*, *116*, A00I22, doi:10.1029/2010JA015762.

Saito, T., and S. Matsushita (1968), Solar cycle effects on geomagnetic Pi2 pulsations, *J. Geophys. Res.*, *73*, 267–286, doi:10.1029/JA073i001p00267.

Saito, T., K. Yumoto, and Y. Koyama (1976a), Magnetic pulsation Pi2 as a sensitive indicator of magnetospheric substorm, *Planet. Space Sci.*, *24*, 1025–1029, doi:10.1016/0032-0633(76)90120-3.

Saito, T., T. Sakurai, and Y. Koyama (1976b), Mechanism of association between Pi2 pulsation and magnetospheric substorm, *J. Atmos. Sol. Terr. Phys.*, *38*, 1265–1277.

Saka, O., O. Watanabe, M. Shinohara, H. Tachihara, and D. N. Baker (1996), A comparison of the occurrence of very-low-latitude Pi2 pulsations with magnetic-field and energetic-particle flux variations (30-300 keV) at geosynchronous altitudes, *J. Geomagn. Geoelectr.*, *48*, 1431–1441.

Sakurai, T., and R. L. McPherron (1983), Satellite observations of Pi 2 activity at synchronous orbit, *J. Geophys. Res.*, *88*, 7015–7027, doi:10.1029/JA088iA09p07015.

Sakurai, T., and T. Saito (1976a), Magnetic pulsations Pi2 and substorm onset, *Planet. Space Sci.*, *24*, 573–575, doi:10.1016/0032-0633(76)90135-5.

Sakurai, T., and T. Saito (1976b), Effect of the substorm phases on the electric field variation near the plasmapause inferred by the pulsation-pearl method, *J. Atmos. Sol. Terr. Phys.*, *38*, 1169–1175.

Sasaki, F., T. Maeda, and M. Yamada (1992), Study of time history data using wavelet transform, *J. Struc. Eng. Architec. Inst. Japan*, *38B*, 9–20, (in Japanese with English abstract).

Sato, K., and M. Yamada (1994), Vertical structure of atmospheric gravity waves revealed by the wavelet analysis, *J. Geophys. Res.*, *99*, 20,623–20,631, doi:10.1029/94JD01818.

Sergeev, V. A., N. P. Dmitrieva, and E. S. Barkova (1986), Triggering of substorm expansion by the IMF directional discontinuities: Time delay analysis, *Planet. Space Sci.*, *34*, 1109–1118, doi:10.1016/0032-0633(86)90023-1.

Singer, H. J., W. J. Hughes, P. F. Fougere, and D. J. Knecht (1983), The localization of Pi 2 pulsations - Ground-satellite observations, *J. Geophys. Res.*, *88*, 7029–7036, doi:10.1029/JA088iA09p07029.

Smith, B. P. (1973), On the occurrence of Pi 2 micropulsations, *Planet. Space Sci.*, *21*, 831–837, doi:10.1016/0032-0633(73)90100-1.

Sutcliffe, P. R., and L. R. Lyons (2002), Association between quiet-time Pi2 pulsations, poleward boundary intensifications, and plasma sheet particle fluxes, *Geophys. Res. Lett.*, *29*, 1293.

Takahashi, K., and K. Liou (2004), Longitudinal structure of low-latitude Pi2 pulsations and its dependence on aurora, *J. Geophys. Res.*, *109*, A12206, doi:10.1029/2004JA010580.

Takahashi, K., K. Liou, and K. Yumoto (2002), Correlative study of ultraviolet aurora and low-latitude Pi2 pulsations, *J. Geophys. Res.*, *107*, 1417, doi:10.1029/2002JA009455.

Verö, J. (1986), Experimental aspects of low-latitude pulsations, A review, *J. Geophys.*, *60*, 106–119.

Yamada, M., and K. Ohkitani (1991), Orthonormal wavelet analysis of turbulence, *Fluid Dyn. Res.*, *8*, 101–115, doi:10.1016/0169-5983(91)90034-G.

Yamanaka, M. D., T. Shimomai, and S. Fukao (1994), A model of quasi-monochromatic field of middle-atmospheric internal gravity waves, in *Proc. of the 1992 STEP Symposium/5th COSPAR Colloquium*, edited by D. N. Baker, V. O. Papitashvili, and M. J. Teague, pp. 511–518.

Yeoman, T. K., M. P. Freeman, G. D. Reeves, M. Lester, and D. Orr (1994), A comparison of midlatitude Pi 2 pulsations and geostationary orbit particle injections as substorm indicators, *J. Geophys. Res.*, *99*, 4085–4093, doi:10.1029/93JA03233.

Yomogida, K. (1994), Detection of anomalous seismic phases by the wavelet transform, *Geophys. J. Int.*, *116*, 119–130, doi:10.1111/j.1365-246X.1994.tb02131.x.

Yumoto, K. (1986), Generation and propagation mechanisms of low-latitude magnetic pulsations, A review, *J. Geophys.*, *60*, 79–105.

Yumoto, K., T. Saito, K. Takahashi, F. W. Menk, B. J. Fraser, T. A. Potemra, and L. J. Zanetti (1989), Some aspects of the relation between Pi1-2 magnetic pulsations observed at L=1.3-2.1 on the ground and substorm-associated magnetic field variations in the near-earth magnetotail observed by AMPTE CCE, *J. Geophys. Res.*, *94*, 3611–3618, doi:10.1029/JA094iA04p03611.

Yumoto, K., et al. (1994), Correlation of high- and low-latitude Pi2 magnetic pulsations observed at 210° Magnetic Meridian Chain stations, *J. Geomagn. Geoelectr.*, *46*, 925–935.

Table 1. Coordinates and Declination of 11 Ground Stations Used in Derivation of the Wp Index[1]

						(degree)
Station	Code	GGLAT[2]	GGLON[2]	GMLAT[3]	GMLON[3]	Declination
Tucson	TUC	32.17	249.27	39.71	316.16	11.1
Honolulu	HON	21.32	202.00	21.51	269.79	10.0
Canberra	CNB	-35.32	149.36	-42.53	226.92	12.6
Kakioka	KAK	36.23	140.19	27.19	208.79	-7.1
Learmonth	LRM	-22.22	114.10	-32.28	186.47	0.5
Urumqi	WMQ	43.80	87.70	33.92	162.21	2.9
Iznik	IZN	40.50	29.73	37.55	109.54	4.2
Fürstenfeldbruck	FUR	48.17	11.28	48.19	94.55	1.5
Ebro	EBR	40.82	0.50	42.99	81.26	-1.2
Tristan da Cunha	TDC	-37.25	347.50	-31.37	53.48	-24.1
San Juan	SJG	18.11	293.85	28.20	6.10	-12.5

[1] Values are calculated for 1 January 2005 by using the 11th Generation IGRF.
[2]GGLAT and GGLON denote geographic latitude and longitude.
[3]GMLAT and GMLON denote geomagnetic latitude and longitude.

Table 2. Comparison Between Wp Enhancements and Substorm Signatures Identified by Other Substorm Indices/Geosynchronous Satellite Data for March 2010

Time of Wp Enhancement (t_0)								Substorm Signatures?	
Date	Time, UT	AE	AL	ASY-H	ASY-D	DRTS	ETS-VIII	Y/Y*	Y/Y*/N*
2010/03/01	2251	N	N	N	N	N	N*		✓
2010/03/02	1105	Y	Y	Y	Y	N*	N	✓	✓
2010/03/02	2137	Y	Y	Y	N	N	N*	✓	✓
2010/03/03	0928	Y	Y	Y	Y	N*	N	✓	✓
2010/03/03	1004	Y	Y	N	Y	N*	Y	✓	✓
2010/03/03	1117	Y	Y	N	Y	N*	Y	✓	✓
2010/03/03	1702	Y	Y	Y	Y	Y	Y	✓	✓
2010/03/04	2014	N	N	N	N	N	N*		✓
2010/03/04	2135	N	N	N	N	N	N*		✓
2010/03/06	0008	Y	Y	Y	N	N*	N*	✓	✓
2010/03/06	1228	Y	Y	N	N	N	N	✓	✓
2010/03/06	1739	N	N	N	N	N	N		
2010/03/07	0519	Y	Y	N	N	N*	N*	✓	✓
2010/03/08	1921	Y	Y	N	N	N	N	✓	✓
2010/03/09	1331	Y	Y	N	N	N	N	✓	✓
2010/03/09	1734	Y	Y	N	N	Y	Y	✓	✓
2010/03/10	1322	Y	Y	Y	Y	Y	Y	✓	✓
2010/03/10	2101	Y	Y	Y	N	N	N*	✓	✓
2010/03/11	0527	Y	Y	Y	Y	Y*	Y*	✓	✓
2010/03/11	0853	Y	Y	N	N	Y*	Y	✓	✓
2010/03/11	1137	Y	Y	N	N	Y*	Y	✓	✓
2010/03/11	1804	Y	Y	Y	N	Y	Y	✓	✓
2010/03/12	0011	Y	Y	Y	Y	N*	N*	✓	✓
2010/03/12	1820	Y	Y	Y	Y	N	N	✓	✓
2010/03/13	1505	Y	Y	Y	N	N	N	✓	✓
2010/03/13	2002	Y	Y	N	N	Y	N*	✓	✓
2010/03/14	0047	Y	Y	Y	N	N*	N*	✓	✓
2010/03/14	1321	Y	Y	Y	Y	Y	Y	✓	✓
2010/03/15	1411	N	N	N	N	N	N		
2010/03/15	1906	Y	Y	N	N	Y	Y	✓	✓
2010/03/16	1251	Y	Y	N	Y	N	Y	✓	✓
2010/03/17	0457	Y	Y	Y	Y	N*	N*	✓	✓
2010/03/17	2024	Y	Y	N	N	N	N*	✓	✓
2010/03/17	2227	Y	Y	Y	Y	N	N*	✓	✓
2010/03/18	1253	N	N	N	N	N	N		
2010/03/18	1900	Y	Y	N	N	N	N	✓	✓
2010/03/18	2211	N	N	N	N	N	N*		✓
2010/03/19	1958	Y	Y	Y	N	N	N	✓	✓
2010/03/19	2119	Y	Y	N	N	N	N*	✓	✓
2010/03/20	0356	Y	Y	Y	N	N*	N*	✓	✓
2010/03/20	1454	N	N	Y	N	N	N	✓	✓
2010/03/20	1547	Y	Y	N	N	Y	Y	✓	✓
2010/03/20	1825	N	N	N	N	Y	Y	✓	✓
2010/03/20	1858	Y	Y	N	N	N	N	✓	✓
2010/03/21	0624	N	N	N	N	N*	N*		✓
2010/03/21	0827	Y	Y	N	N	N*	N	✓	✓
2010/03/21	1016	N	N	N	N	N*	N		✓
2010/03/21	1416	Y	N	N	N	N	N	✓	✓
2010/03/21	1501	N	N	N	N	N	N		
2010/03/21	1732	N	N	N	N	N	N		
2010/03/21	2055	N	N	N	N	N	N*		✓
2010/03/21	2128	N	N	N	N	N	N*		✓

2010/03/24	1209	N	N	N	Y	N	N	✓	✓
2010/03/24	2157	Y	Y	Y	N	N	N*	✓	✓
2010/03/25	1413	Y	Y	N	N	N	Y	✓	✓
2010/03/25	1759	Y	Y	N	Y	Y	Y	✓	✓
2010/03/26	1137	Y	Y	N	Y	Y*	Y	✓	✓
2010/03/28	0438	Y	Y	N	N	N*	N*	✓	✓
2010/03/28	1336	N	N	N	N	Y	Y	✓	✓
2010/03/28	1541	Y	Y	N	N	Y	N	✓	✓
2010/03/28	2323	N	N	N	N	N	N*		✓
2010/03/29	0230	N	N	Y	N	Y*	Y*	✓	✓
2010/03/29	1026	Y	Y	N	N	N*	N	✓	✓
2010/03/30	1810	Y	Y	Y	N	N	N	✓	✓

Y, yes; N, no; *, Satellite on dayside.

Table 3. Number of Events in Each Classification Category

Category	AE	AL	ASY-H	ASY-D	DRTS	ETS-VIII
Y	45	44	22	16	12	17
Y*	-	-	-	-	5	2
N	19	20	42	48	32	23
N*	-	-	-	-	15	22

Table 4. Comparison Between AE and Wp Enhancements for March 2010

Time of AE Enhancement (t_0')		
Date	Time, UT	Wp
2010/03/01	1227	B
2010/03/02	1109	A
2010/03/03	0928	A
2010/03/05	1750	B
2010/03/05	2358	A
2010/03/08	1437	C
2010/03/08	1921	A
2010/03/12	0020	A
2010/03/12	0834	B
2010/03/14	0741	B
2010/03/14	1323	A
2010/03/16	1306	A
2010/03/17	0451	A
2010/03/20	0702	A
2010/03/20	0709	A
2010/03/20	1351	A
2010/03/24	1413	B
2010/03/25	1437	A
2010/03/26	1143	A
2010/03/28	0344	B
2010/03/28	1138	B
2010/03/28	1146	B
2010/03/29	1547	A
2010/03/29	2316	A

Peak Value of Wp: A, $\geq$0.4 nT; B, $\geq$0.2 nT and $<$0.4 nT; C, $<$0.2 nT

Figure 1. Location of 11 ground stations used to derive the Wp index in geomagnetic coordinates. Dotted blue circles indicate geomagnetic latitudes of 20° and 50°.

Figure 2. Schematic figure of the derivation procedure for the Wp index. Details are described in the text.

Figure 3. The 1-s geomagnetic field data in the H_N component from the 11 stations for time intervals of (a) 0500-0600 UT, (b) 0820-0920 UT, (c) 1110-1210 UT, and (d) 1740-1840 UT on 11 March 2010. MLT of each station at the beginning of the time interval is indicated at the bottom-left corner of each panel.

Figure 4. (1st to 11th panels) The W_{ABB} indices of 11 stations for 11 March 2010. A horizontal black bar in each panel indicates local nighttime (1800-0400 MLT) of the station. Horizontal light-blue bars indicate the four time intervals shown in Figure 3. (12th panel) The Wp index for 11 March 2010 calculated from W_{ABB} shown in the 1st to 11th panels. Horizontal light-blue bars represent the same time intervals as above.

Figure 5. Stack plots for 11 March 2010 showing the AE, -AL, ASY-H, ASY-D, and Wp indices, the high-energy (590-1180 keV) electron flux measured by the DRTS geosynchronous satellite, and the magnetic field in the *PEN* coordinates measured by the ETS-VIII geosynchronous satellite.

Supplemental Figure 1. One-second geomagnetic field data from the 11 Wp stations for Event 1-4.
Supplemental Figure 2. One-second geomagnetic field data from the 11 Wp stations for Event 5-8.
Supplemental Figure 3. One-second geomagnetic field data from the 11 Wp stations for Event 9-12.
Supplemental Figure 4. One-second geomagnetic field data from the 11 Wp stations for Event 13-14.

Figure 1

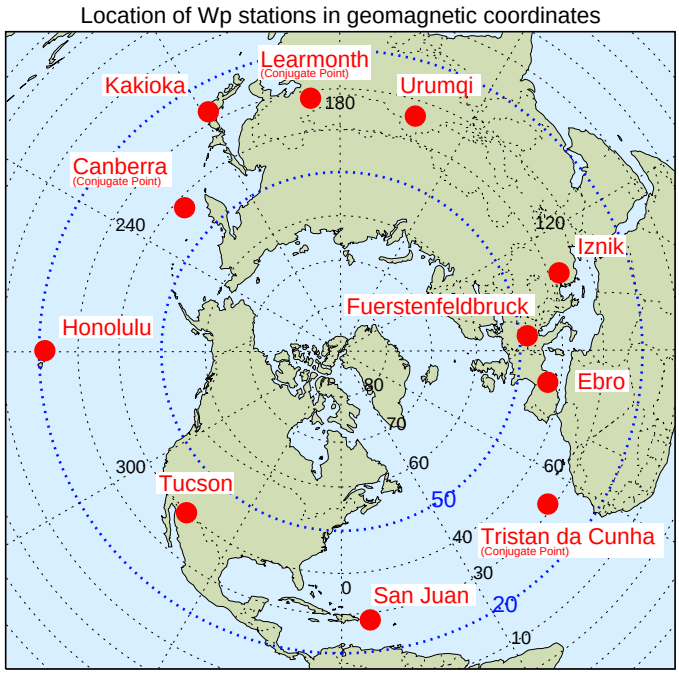

Figure 2

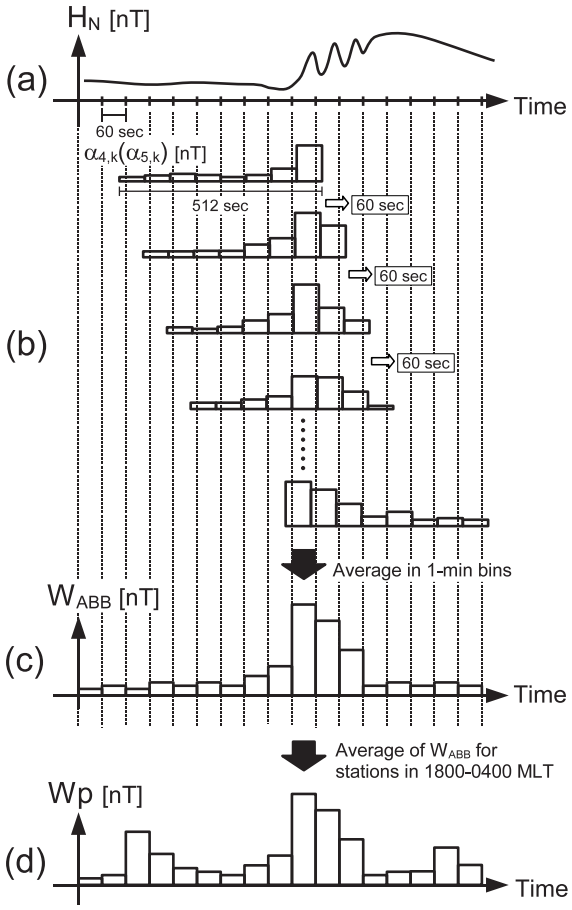

Figure 3

Figure 4

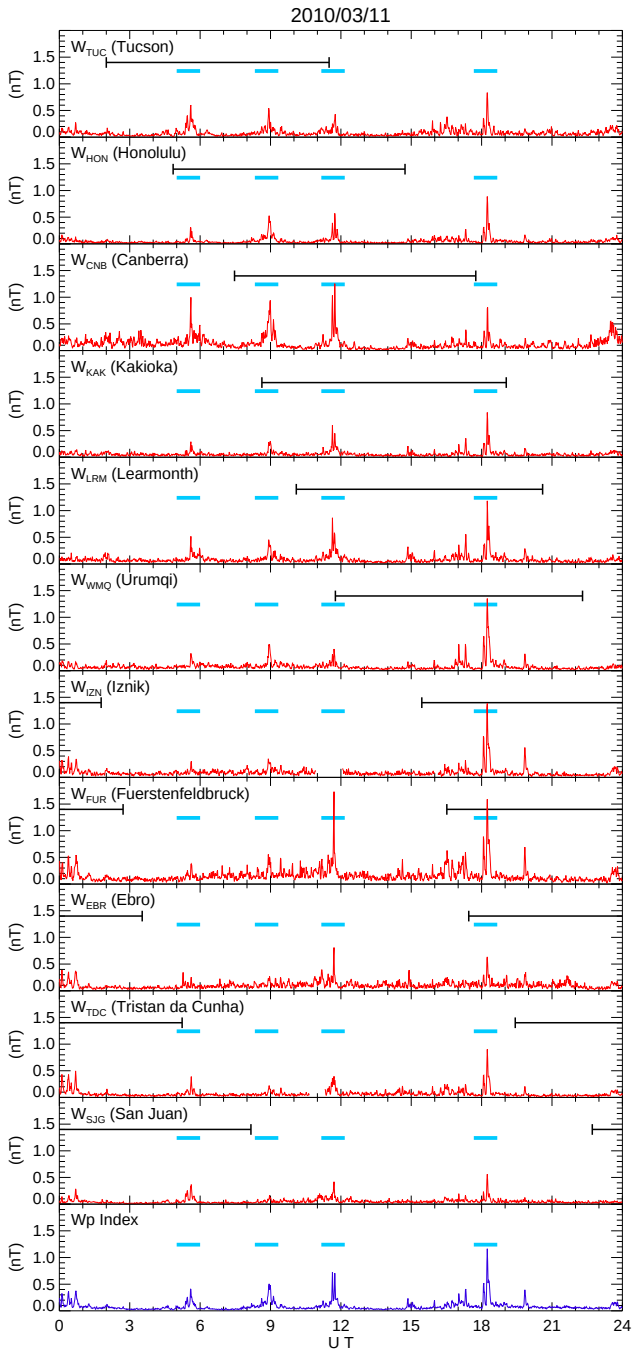

Figure 5

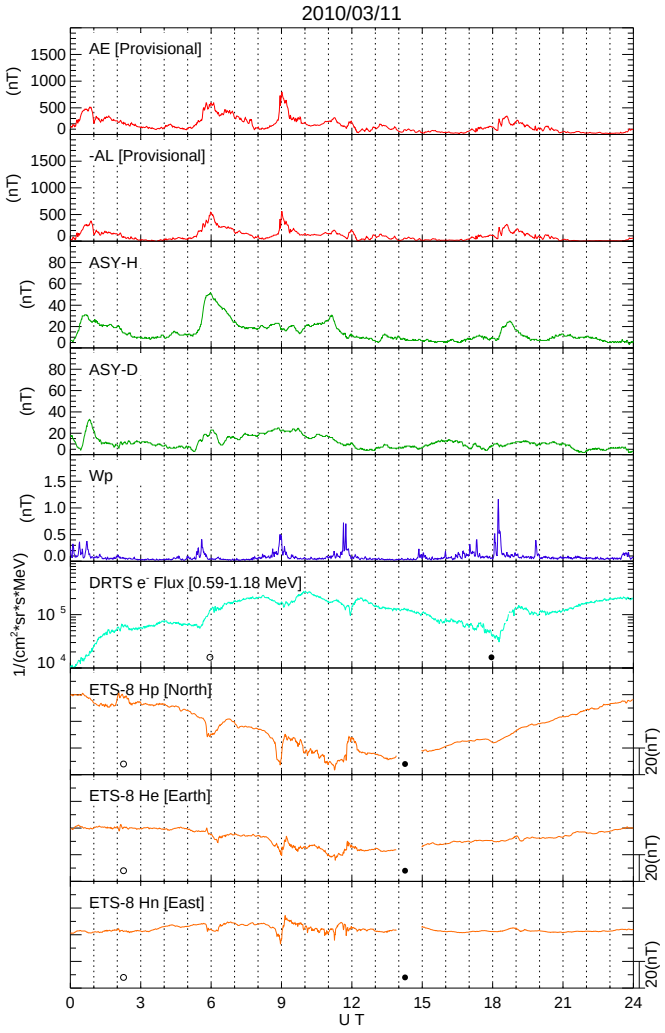

Supplemental Figure 1

Supplemental Figure 2

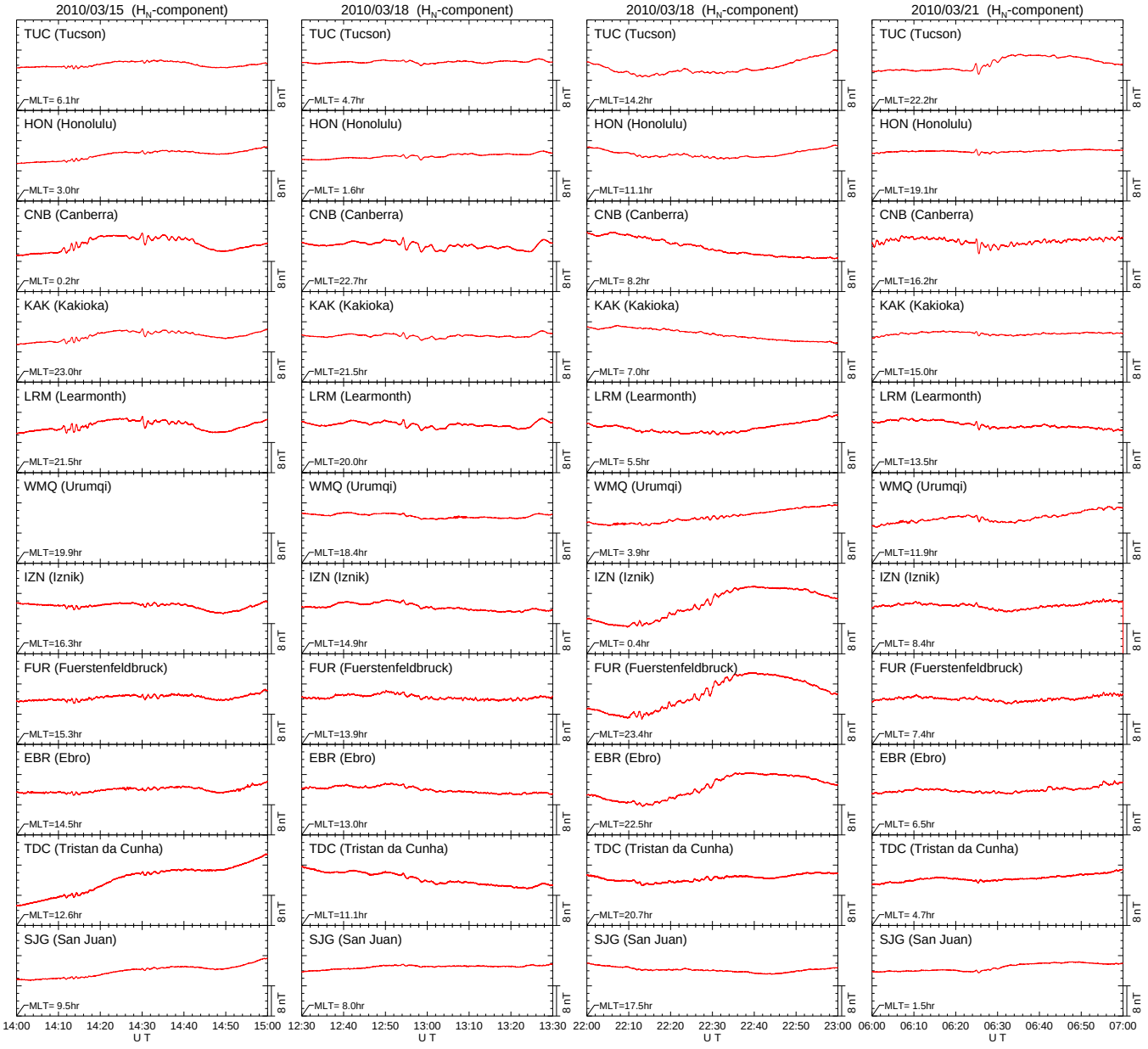

Supplemental Figure 3

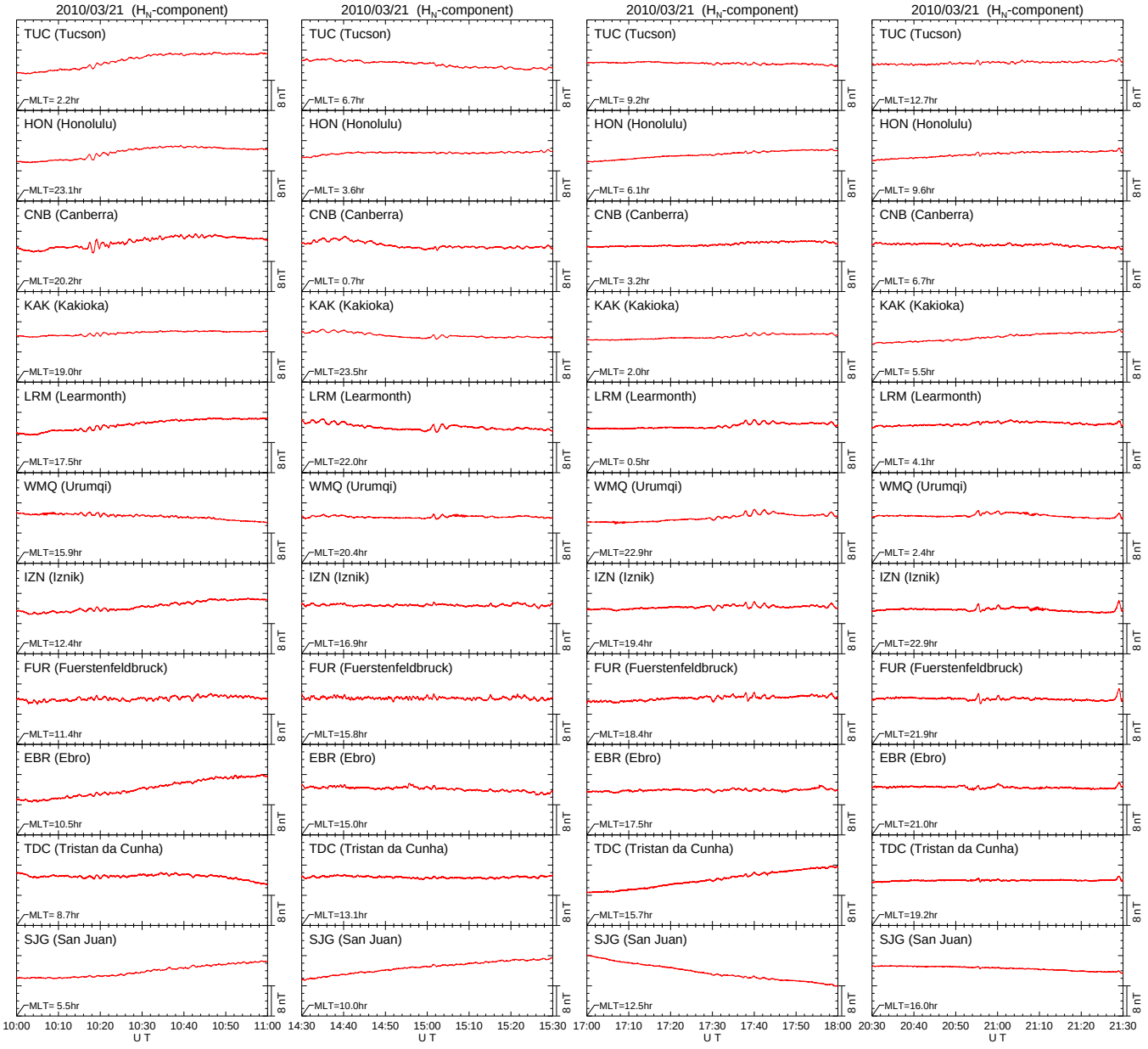

Supplemental Figure 4